

Melatonin Suppresses NLRP3 Inflammasome Activation via SIRT1-Mediated ETS1 Deacetylation to Attenuate LPS-Induced Pyroptosis in Alveolar Epithelial Cells

Fan He, Chunzi Liu, Yun Yu, Qiaofang Wang, Lin Li, Xiaoyun Chao, Liping Chen, Cong Yu

Neonatal Intensive Care Unit, Jiangxi Provincial Children's Hospital, Nanchang, Jiangxi, 330038, People's Republic of China

Correspondence: Liping Chen; Cong Yu, Neonatal Intensive Care Unit, Jiangxi Provincial Children's Hospital, No. 1666, DieziHu Road, Honggutan District, Nanchang, Jiangxi, 330038, People's Republic of China, Tel + 86 13627918180, Email cclpp88@qq.com; yucong@ncmc.edu.cn

Purpose: While melatonin is known to suppress pyroptosis in various cell types, its role and mechanisms in alveolar epithelial cells are not fully understood. Using lipopolysaccharide (LPS)-treated human pulmonary alveolar epithelial cells (HPAEpiC) as an in vitro model, this study aimed to investigate the anti-pyroptotic mechanism of melatonin.

Methods: HPAEpiC cells were treated with LPS to induce pyroptosis. Cell death was assessed by propidium iodide staining, and morphological changes were examined using transmission electron microscopy (TEM). Pyroptosis-related markers were analyzed by Western blot and immunofluorescence, while inflammatory factors were measured by enzyme-linked immunosorbent assay (ELISA). Chromatin immunoprecipitation (ChIP) assay and siRNA knockdown were performed to identify key targets and mechanisms involved in melatonin-mediated inhibition of pyroptosis.

Results: Melatonin significantly reduced LPS-induced pyroptosis in HPAEpiC cells. It downregulated the expression of E26 oncogene homolog 1 (ETS1), and overexpression of ETS1 reversed the anti-pyroptotic effect of melatonin. ChIP assays confirmed that ETS1 binds to the NLRP3 promoter, an interaction inhibited by melatonin. Additionally, melatonin upregulated sirtuin 1 (SIRT1), leading to ETS1 deacetylation. Knockdown of SIRT1 abolished the protective effect of melatonin against pyroptosis. Furthermore, siRNA targeting melatonin receptor 2 (MT2) attenuated melatonin-induced SIRT1 upregulation, ETS1 deacetylation, and pyroptosis inhibition.

Conclusion: Our findings indicate that melatonin alleviates LPS-induced pyroptosis in alveolar epithelial cells through the MT2/SIRT1/ETS1/NLRP3 signaling pathway.

Keywords: melatonin, LPS, ETS1, SIRT1, pyroptosis, pulmonary alveolar epithelial cells

Introduction

Alveolar epithelial cells (ACEs) are pivotal for maintaining pulmonary structural and functional integrity.^{1,2} Damage and death of these cells, triggered by viral infection, bacterial toxins, hypoxia, or mechanical stress, constitute key determinants in the progression and severity of acute lung injury (ALI) and its more severe form, acute respiratory distress syndrome (ARDS).^{1,2} While apoptosis has long been recognized as a primary mechanism underlying alveolar epithelial injury, its characteristically intact plasma membrane and limited inflammatory response fail to account for the pronounced inflammatory cascade observed in ALI/ARDS. Recent evidence highlights the importance of pyroptosis, a lytic and highly inflammatory form of programmed cell death, in the pathogenesis of lipopolysaccharide (LPS)-induced lung injury.³⁻⁵ In contrast to apoptosis, pyroptosis is typically mediated by inflammasome activation, such as the NLRP3 (NOD-like receptor family pyrin domain-containing 3) inflammasome, leading to gasdermin D-mediated pore formation, cytokine release, and robust inflammation.⁶ LPS has demonstrated to be one of the most common triggers of pyroptosis

of ACEs.^{1,7,8} Thus, targeting LPS-induced pyroptosis in these cells may hold clinical promise for the management of lung injury.

Melatonin, a neuroendocrine hormone chiefly synthesized by the pineal gland, possesses diverse biological properties, including antioxidant, anti-aging, immunomodulatory, and anticancer effects. It has shown therapeutic potential in various conditions such as cancer, Alzheimer's disease (AD), and heart failure.^{9,10} In pulmonary diseases, melatonin exhibits protective effects in experimental models of acute lung injury, ischemia-reperfusion injury, and chronic obstructive pulmonary disease.^{11–13} Notably, emerging studies indicate that melatonin can suppress pyroptosis in several cellular contexts, though its anti-pyroptotic mechanisms appear to be cell- and stimulus-dependent.^{13–17} Despite these advances, the precise role and molecular pathways through which melatonin modulates pyroptosis in alveolar epithelial cells remain unclear.

ETS1, a member of the ETS family of transcription factors, is expressed in ACEs and other cell types,¹⁸ where it regulates proliferation, differentiation, and apoptosis.^{19–21} Recent work demonstrated that ETS1 knockdown mitigates pyroptosis in renal tubular epithelial cells,²² suggesting a broader role in inflammatory cell death. Furthermore, we previously identified ETS1 as a downstream effector of melatonin in protecting alveolar epithelial type II cells against hyperoxia-induced apoptosis.²³

Building on these observations, we hypothesized that ETS1 may also mediate the anti-pyroptotic action of melatonin in AECs. In this study, we tested this hypothesis and delineated a signaling axis, MT2/SIRT1/ETS1/NLRP3, through which melatonin alleviates LPS-induced pyroptosis in human pulmonary alveolar epithelial cells (HPAEPiC).

Materials and Methods

Cell Culture and Treatment

Human pulmonary alveolar epithelial cells (HPAEPiC; Cat. No. 3200) and the human normal liver L-02 cell line (Cat. No. ZQ0031) were obtained from Shanghai Zhong Qiao Xin Zhou Co., Ltd. (Shanghai, China). Cell identity was authenticated by short tandem repeat (STR) profiling upon receipt and was routinely confirmed to be free of mycoplasma contamination. HPAEPiC cells were maintained in Alveolar Epithelial Cell Medium (Cat. No. 3201; Zhong Qiao Xin Zhou) supplemented with 10% fetal bovine serum (FBS; Cat. No. 0010; Zhong Qiao Xin Zhou), 1% Epithelial Cell Growth Supplement (Cat. No. 4152; Zhong Qiao Xin Zhou), and 1% penicillin/streptomycin (Cat. No. 0503; Zhong Qiao Xin Zhou). L-02 cells were cultured in Roswell Park Memorial Institute-1640 (RPMI-1640; Cat. No. ZQ-200; Zhong Qiao Xin Zhou) containing 10% FBS and 1% penicillin/streptomycin. All cells were incubated at 37°C in a humidified atmosphere with 5% CO₂. All experiments were performed using cells within passage numbers 15 to 25 to ensure phenotypic stability. For experimental treatments, HPAEPiC cells were pretreated with varying concentrations of melatonin (Cat. No. HY-B0075; MedChemExpress, USA) for 1 hour, followed by exposure to LPS (100 ng/mL; Cat. No. L4391; Sigma-Aldrich Co., USA) for 24 hours. Subsequently, the culture medium and cellular proteins were collected for further analysis.

Plasmid, siRNA and Cell Transfection

ETS1 overexpression was achieved using the pcDNA3.1-HA plasmid (Jinsite Biotechnology, Nanjing, China). Small-interfering RNAs (siRNAs) targeting ETS1, MT1, MT2, SIRT1, SIRT6, and SIRT7, along with a negative control siRNA, were designed and synthesized by GenePharm (Shanghai, China). The siRNA sequences used were as follows: ETS1, 5'-ACUUGCUACCAUCCCGUAC-3'; MT1, 5'-GGUGUCCAUUUCAUAGU-3'; MT2, 5'-GGAGCUUUCUGAGCAUGU-3'; SIRT1, 5'-CCCUCAAAGUAAGACCAGUTT-3'; SIRT6, 5'-GAAUGUGCCAAGUGUAAGATT-3'; SIRT7, 5'-CUGUGUUGCUGAGGAUAATT-3'; and control siRNA, 5'-UUCUCCGAACGUGUCACGUTT-3'. Cell transfection was performed using Lipofectamine 2000 (Invitrogen) according to the manufacturer's protocol. After 24 hours of transfection, cells were subjected to further treatments or harvested for subsequent assays. Knockdown efficiency was assessed via Western blot analysis.

Cell Viability Analysis

Cell viability was assessed using the Cell Counting Kit-8 (CCK-8) assay. HPAEpiC cells were seeded into 96-well plates at a density of 1×10^4 cells per well. Following the indicated treatments, the culture medium was replaced with 80 μ L of fresh medium containing 20 μ L of CCK-8 reagent (Cat. No. C0038; Beyotime, Shanghai, China). The absorbance at 450 nm was measured using a microplate reader (ELx800; BioTek Instruments, Inc., Winooski, VT, USA). Cell viability was expressed as a percentage relative to the control group.

Hoechst33342/PI Staining

HPAEpiC cells were seeded in 12-well plates at a density of 10^5 cells per well and treated as described. After treatment, cells were washed three times with PBS and stained with Hoechst 33342/PI (Cat. No. C1056; Beyotime) for 30 minutes at 4°C in the dark. Stained cells were visualized using a fluorescence microscope (Leica DM2500; Wetzlar, Germany).

Enzyme-Linked Immunosorbent Assay (ELISA)

The concentrations of IL-1 β and IL-18 in the cell culture supernatants were measured using commercial ELISA kits (Beyotime, Shanghai, China) according to the manufacturer's instructions. The following kits were used: IL-1 β (Cat. No. PI305) and IL-18 (Cat. No. PI558).

Immunofluorescence Staining

After treatment, HPAEpiC cells were fixed with 4% paraformaldehyde, permeabilized with 0.1% Triton X-100, and blocked with 1% BSA for 1 hour at room temperature. Cells were then incubated overnight at 4°C with primary antibodies against ETS1 (1:100; Cat. No. A15666; ABclonal, Wuhan, China) or caspase-1 (1:100; Cat. No. A0964; ABclonal). After washing, cells were incubated with appropriate secondary antibodies for 1 hour at room temperature. Nuclei were counterstained with 4',6-diamidino-2-phenylindole (DAPI; Sigma-Aldrich). Images were acquired using a fluorescence microscope (Leica DM2500).

Western Blot Analysis

Cells were lysed, and Western blotting was performed as previously described.²³ The following primary antibodies were used: anti-cleaved caspase-1 (1:1000; Cat. No. #4199; Cell Signaling Technology, MA, USA), anti-MT2 (1:1000; Cat. No. ab203346; Abcam, Cambridge, UK), anti-ETS1 (1:1000; Cat. No. A19603; ABclonal), anti-GAPDH (1:10,000; Cat. No. A19056; ABclonal), anti-NLRP3 (1:1000; Cat. No. A5652; ABclonal), anti-GSDMD-N (1:1000; Cat. No. A22523; ABclonal), anti-SIRT1 (1:500; Cat. No. A19667; ABclonal), anti-SIRT6 (1:2000; Cat. No. A3591; ABclonal), anti-SIRT7 (1:2000; Cat. No. A22735; ABclonal), anti- α -Tubulin (1:5000; Cat. No. AC012; ABclonal), anti-Histone H3 (1:5000; Cat. No. A2348; ABclonal), anti-MT1 (1:2000; Cat. No. A13030; ABclonal), and pan-acetyl-lysine (1:1000; Cat. No. A1525; ABclonal).

Quantitative Real-Time PCR (qRT-PCR)

Total RNA was extracted from HPAEpiC cells using TRIzol reagent. After chloroform extraction and isopropanol precipitation, RNA was reverse-transcribed into cDNA using a reverse transcriptase kit (Cat. No. #RR036A; Takara Ltd., Otsu, Japan). Quantitative PCR was performed using TB Green Premix Ex Taq II (Cat. No. #RR820A; Takara Ltd) on an ABI 7300 real-time PCR system (Applied Biosystems Inc). GAPDH was used as an internal control. The primer sequences were as follows: NLRP3 forward, 5'-GATGGGTCAAGATGGCATCG-3', and reverse, 5'-AAGTTCTCCTGTTGGCTCGA-3'; GAPDH forward, 5'-CGGAGTCAACGGATTGGTCGTAT-3', and reverse, 5'-AGCCTTCTCCATGGTGGTGAAGAC-3'.

Chromatin Immunoprecipitation (ChIP) Assay

A ChIP assay was conducted using a commercial kit (Cat. No. P2078; Beyotime) to examine the binding of ETS1 to the NLRP3 promoter. HPAEpiC cells were cross-linked with 1% formaldehyde for 10 minutes, and the reaction was quenched with glycine (0.125 mol/L). After washing with ice-cold PBS, cells were lysed and subjected to sonication. Cell lysates were incubated overnight at 4°C with magnetic beads conjugated to anti-ETS1 (Cat. No. #14069; Cell

Signaling Technology) or anti-IgG (Cat. No. A7016; Beyotime). The isotype-matched normal IgG was used as a negative control. Following cross-link reversal and DNA purification, the enriched DNA was analyzed by qPCR using the following primers: forward, 5'-CGAGACACGGTTTTGACA-3', and reverse, 5'-ACACTGCCCCGCGGAGCT-3'. The qPCR primers for the *NLRP3* promoter were designed to flank predicted ETS1 transcription factor binding sites identified using the JASPAR database (<http://jaspar.genereg.net/>). The primer sequences amplify a region upstream of the transcription start site, which contains a conserved ETS1-binding motif.

Transmission Electron Microscopy

Cells were fixed with 2.5% glutaraldehyde for 4 h at 25 °C and subsequently centrifuged at 800 rpm for 5 min to form compact cell pellets. The pellets were then embedded in 1% agarose, washed three times with 0.1 M phosphate buffer (pH 7.4), and post-fixed with 1% osmium tetroxide for 1–2 h. After dehydration through a graded ethanol series, the samples were infiltrated and embedded in epoxy resin. Ultrathin sections (70–90 nm) were cut using an ultramicrotome, double-stained with uranyl acetate (2% saturated solution in ethanol) and lead citrate, and dried overnight at 25 °C. Finally, cellular morphology and ultrastructural details were examined using a Hitachi 800 transmission electron microscope (Tokyo, Japan).

Statistical Analysis

Data are expressed as mean \pm standard deviation (SD) from at least three independent experiments. Statistical analyses were conducted using GraphPad Prism software (version 10.0, USA). Normality of data distribution was assessed using the Shapiro–Wilk test. For normally distributed data, parametric tests were employed: the unpaired Student's *t*-test was used for comparisons between two groups, and one-way or two-way ANOVA followed by Tukey's honestly significant difference (HSD) post hoc test was applied for comparisons among more than two groups. When multiple groups were compared against a single control group, Dunnett's test was used after ANOVA. For data that did not meet the assumption of normality, non-parametric tests were used: the Mann–Whitney *U*-test for two-group comparisons and the Kruskal–Wallis test followed by Dunn's post hoc test for multiple groups. A *p*-value < 0.05 was considered statistically significant.

Results

Melatonin Suppresses LPS-Induced Pyroptosis in HPAEpiC Cells

To investigate the effect of melatonin on LPS-induced pyroptosis in human pulmonary alveolar epithelial cells (HPAEpiCs), cells were treated with increasing concentrations of melatonin. Treatment with melatonin alone for 24 h showed no significant effect on cell viability (Figure 1A). In contrast, melatonin restored the viability of LPS-exposed HPAEpiC cells in a concentration-dependent manner (Figure 1B). The maximum protective effect was achieved at 200 μ M, which was therefore used in subsequent experiments. Hoechst33342/PI staining showed that LPS exposure markedly increased the number of PI-positive cells, an effect that was significantly reduced by co-treatment with 200 μ M melatonin (Figure 1C). Moreover, melatonin substantially attenuated the LPS-induced increase in cleaved caspase-1 (c-caspase-1) fluorescence intensity (Figure 1D). Western blot analysis further demonstrated that melatonin down-regulated the protein expression of key pyroptosis-related mediators, including NLRP3, c-caspase-1, and the N-terminal fragment of GSDMD (GSDMD-N), in LPS-stimulated cells (Figure 1E). Consistent with these results, ELISA assays revealed that melatonin significantly inhibited the LPS-induced secretion of the pro-inflammatory cytokines IL-1 β and IL-18 into the cell culture supernatant (Figure 1F). Pyroptosis is characterized by membrane pores formation. A transmission electron microscope was used to observe ultrastructural damages in HPAEpiC cells. As shown in Figure 1G, we observed bubbles and large holes in the plasma membrane of HPAEpiC cells from the LPS group, in contrast to the linear and intact plasma membrane from the control group. Notably, melatonin treatment appeared to mitigate these changes. Taken together, these findings demonstrate that melatonin effectively suppresses LPS-induced pyroptosis in HPAEpiC cells.

Melatonin Inhibits LPS-Induced Pyroptosis in HPAEpiC Cells by Downregulating ETS1

Based on prior findings that identified E26 oncogene homolog 1 (ETS1) as a downstream target of melatonin in alveolar epithelial type II cells (AECIIs),²³ and its key role in regulating pyroptosis in epithelial cells,²² we investigated whether ETS1 mediates the anti-pyroptotic effects of melatonin in LPS-exposed HPAEpiC cells. LPS treatment elevated ETS1 protein levels, which was suppressed by melatonin co-treatment (Figure 2A). Immunofluorescence analysis further

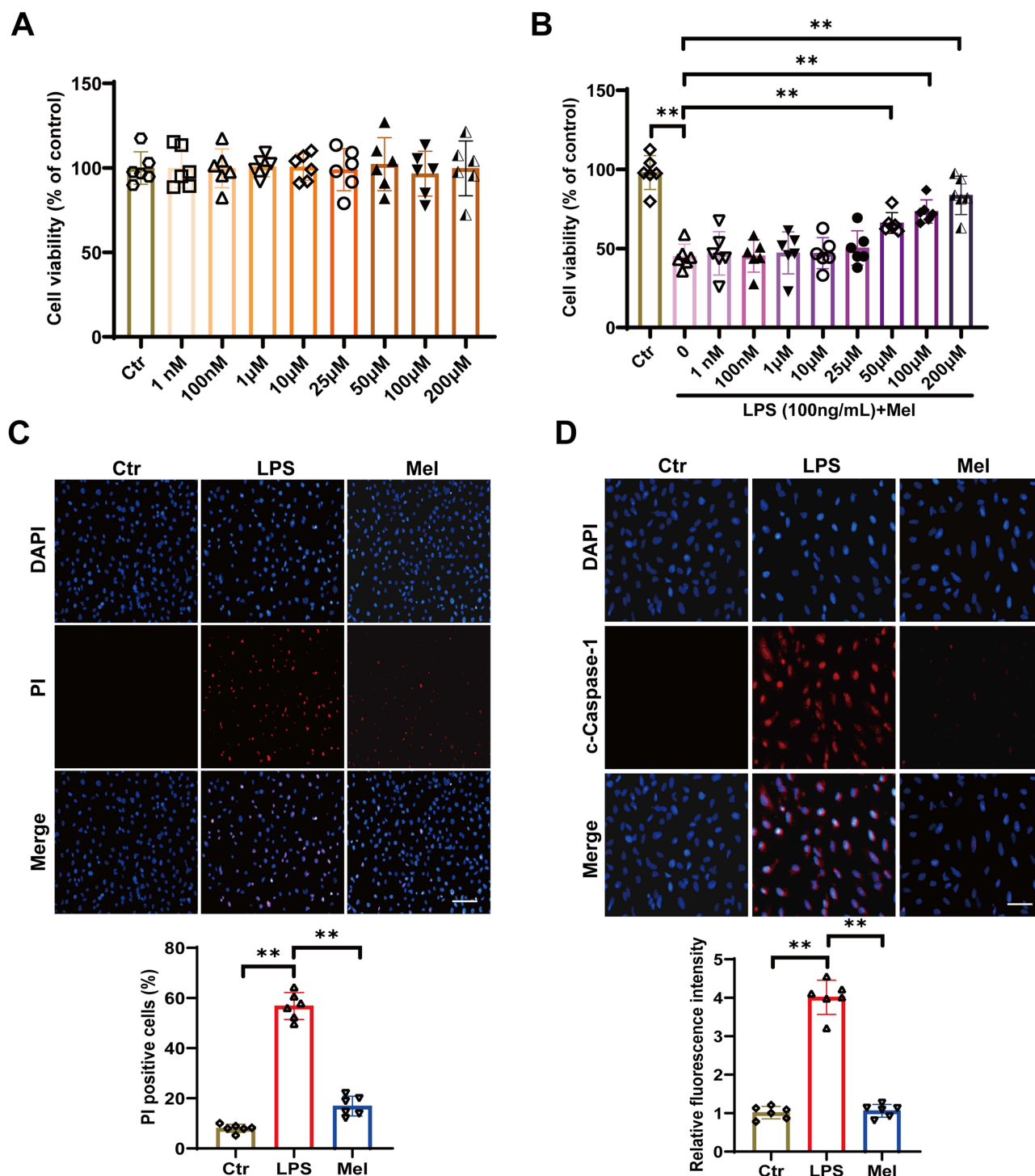
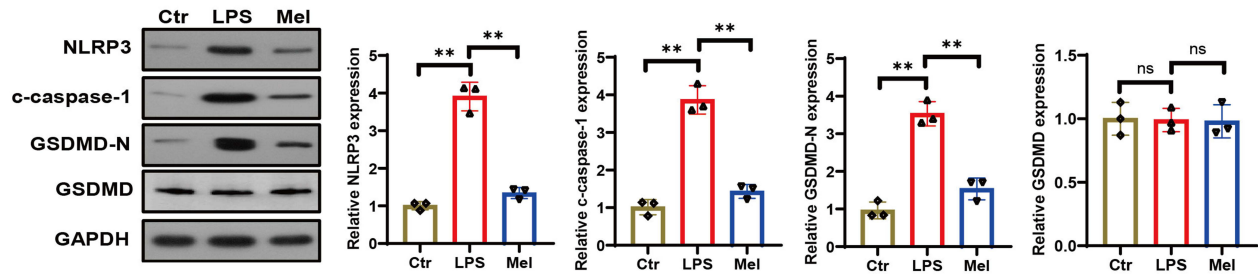
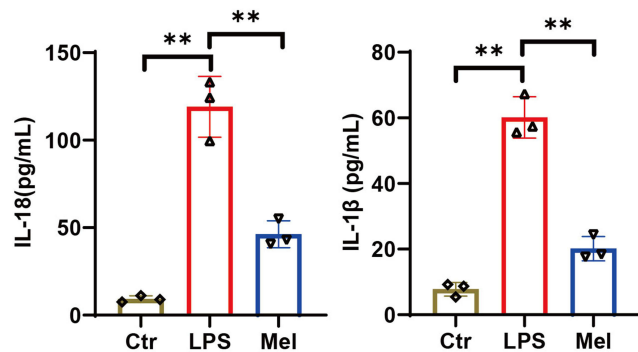


Figure 1 Continued.

E



F



G

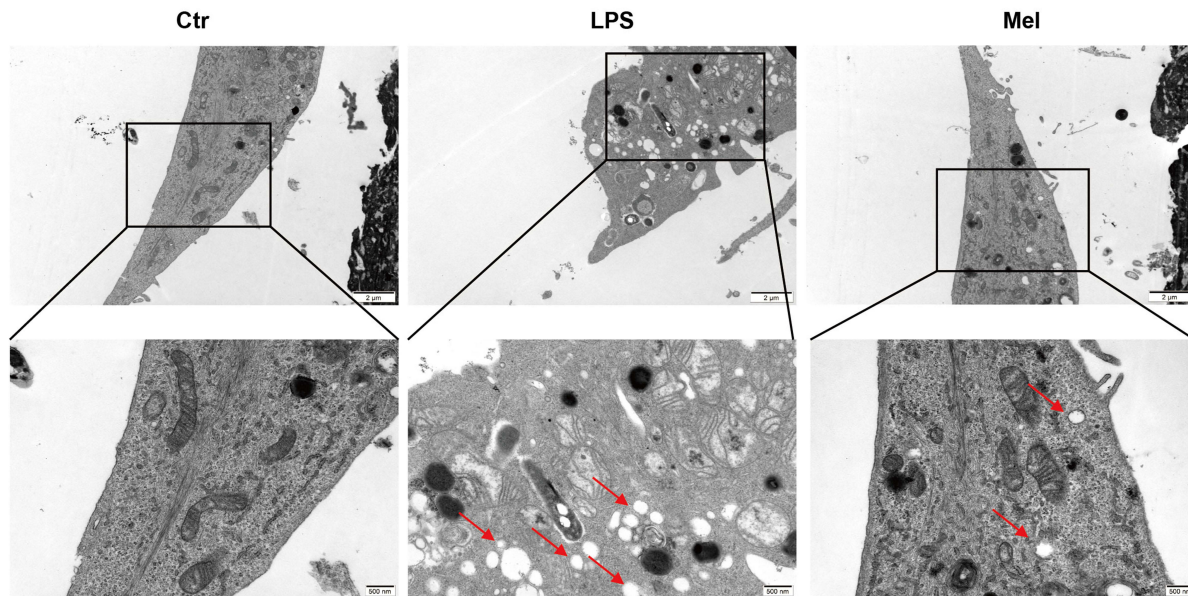


Figure 1 The effect of melatonin on LPS-induced pyroptosis in HPAEpiC cells. **(A)** HPAEpiC cells were treated with different concentrations of melatonin. After 24 h of treatment, cell viability was determined by the CCK-8 assay. n=6. Data are shown as mean ± SD. **P<0.01. One-way ANOVA and Tukey's test. **(B)** HPAEpiC cells were treated with LPS alone or pre-treated with different concentrations of melatonin for 1 h and then treated with LPS (100 ng/mL) for 24 h, cell viability was determined by the CCK-8 assay. n=6. Data are shown as mean ± SD. **P<0.01. One-way ANOVA and Tukey's test. **(C)** Hoechst33342/PI staining analysis of apoptosis in control (ctr), LPS- or LPS + melatonin (Mel)-treated HPAEpiC cells. Scale bar=100 μm. Low panel: Quantification of PI-positive cells. Six regions were randomly selected for each group. Data are shown as mean ± SD. **P<0.01. One-way ANOVA and Tukey's test. **(D)** Immunofluorescence analysis of the levels of cleaved caspase-1 (c-caspase-1) in control (ctr), LPS- or LPS + melatonin (Mel)-treated HPAEpiC cells. Scale bar: 50μm. Low panel: Quantification of c-caspase-1 IF intensity. Six regions were randomly selected for each group, and the IF intensity of c-caspase-1 was quantified using the Imagej software. Data are shown as mean ± SD. **P<0.01. One-way ANOVA and Tukey's test. **(E)** Western blot analysis of NLRP3, c-caspase-1, GSDMD-N and GSDMD in control (ctr), LPS- or LPS + melatonin (Mel)-treated HPAEpiC cells. Data are shown as mean ± SD. n=3 **P<0.01, ns, no significant. One-way ANOVA and Tukey's test. **(F)** ELISA analysis of supernatant levels of IL-1β and IL-18 in control (ctr), LPS- or LPS + melatonin (Mel)-treated HPAEpiC cells. Data are shown as mean ± SD. **P<0.01. One-way ANOVA and Tukey's test. **(G)** Transmission electron microscopy (TEM) images of HPAEpiC cells from different treatment groups. Red arrowheads indicate the large bubbles emerging from the plasma membrane. The scatter points (circles, diamonds, squares, triangles) on each data group of the bar chart represent individual data points.

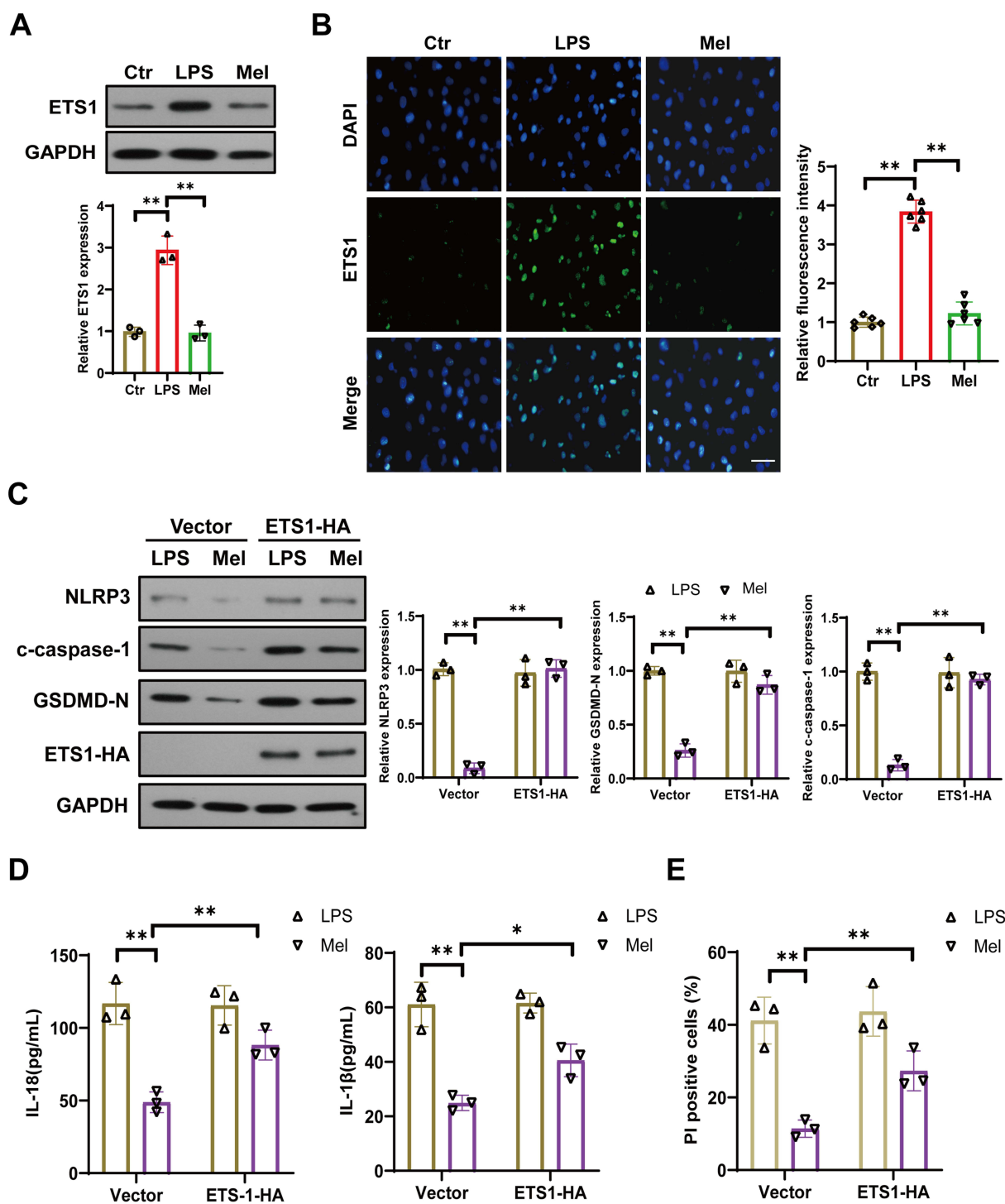


Figure 2 ETS1 mediates the anti-pyrototic effect of melatonin in LPS-exposed HPAEpiC cells. **(A)** Western blot analysis of ETS1 in control (ctr), LPS- or LPS + melatonin (Mel)-treated HPAEpiC cells. Data are shown as mean \pm SD. $n=3$. $**P<0.01$. One-way ANOVA and Tukey's test. **(B)** Immunofluorescence analysis of the levels of ETS1 in control (ctr), LPS- or LPS + melatonin (Mel)-treated HPAEpiC cells. Scale bar: $50\mu\text{m}$. Right panel: Quantification of ETS1 IF intensity. Six regions were randomly selected for each group, and the IF intensity of ETS1 was quantified using the ImageJ software. Data are shown as mean \pm SD. $**P<0.01$. One-way ANOVA and Tukey's test. **(C)** Western blot analysis of NLRP3, c-caspase-1, and GSDMD-N in cells treated with LPS or LPS + melatonin (Mel), transfected with empty plasmid (vector) or ETS1 overexpression plasmid (ETS1-HA). Data are shown as mean \pm SD. $n=3$. $**P<0.01$. Two-way ANOVA and Tukey's test. **(D)** ELISA analysis of supernatant levels of IL-1 β and IL-18 in culture supernatants from the same experimental groups. Data are shown as mean \pm SD. $n=3$. $*P<0.01$, $**P<0.01$. Two-way ANOVA and Tukey's test. **(E)** Hoechst33342/PI staining analysis of apoptosis under the same conditions. Data are shown as mean \pm SD. $n=3$. $**P<0.01$. Two-way ANOVA and Tukey's test. The scatter points (circles, diamonds, triangles) on each data group of the bar chart represent individual data points.

showed that melatonin reduced the nuclear accumulation of ETS1 in LPS-stimulated cells (Figure 2B). Notably, overexpression of ETS1 largely reversed the melatonin-induced decrease in protein levels of NLRP3, c-caspase-1, and GSDMD-N (Figure 2C), as well as the releases of IL-1 β and IL-18 (Figure 2D), and the proportion of PI-positive cells (Figure 2E). Together, these data indicate that melatonin attenuates LPS-induced pyroptosis in HPAEpiC cells through downregulation of ETS1.

ETS1 Mediates the Anti-Pyroptotic Effect of Melatonin by Directly Regulating NLRP3 Expression

To determine whether NLRP3, a core inflammasome component in pyroptosis, serves as a direct transcriptional target of ETS1 in our model, we first examined NLRP3 expression in LPS-exposed HPAEpiC cells. Both NLRP3 mRNA and protein levels were significantly elevated following LPS stimulation (Figure 3A and B). Knockdown of ETS1 by siRNA markedly attenuated these LPS-induced increases in NLRP3 expression at the mRNA and protein levels (Figure 3A and B). Similarly, treatment with melatonin reduced the upregulation of NLRP3 mRNA (Figure 3C) and protein (Figure 1E) in LPS-stimulated cells. Bioinformatic analysis identified two potential ETS1-binding sites within the NLRP3 promoter region (Figure 3D). Chromatin immunoprecipitation (ChIP) assays confirmed that ETS1 directly binds to these promoter sites (Figure 3E), supporting its role in transcriptional regulation. Notably, the enhanced binding of ETS1 to the NLRP3 promoter induced by LPS was significantly suppressed by melatonin treatment (Figure 3E). Collectively, these results demonstrate that ETS1 mediates the anti-pyroptotic effect of melatonin by directly binding to the NLRP3 promoter and regulating its transcription in LPS-exposed HPAEpiC cells.

Melatonin Promotes ETS1 Deacetylation via Sirt1 in LPS-Exposed HPAEpiC Cells

Given the critical role of ETS1 acetylation in regulating its transcriptional activity,²⁴ we examined whether melatonin influences ETS1 acetylation. In HPAEpiC cells, LPS exposure markedly increased ETS1 acetylation, an effect that was substantially attenuated by melatonin treatment, indicating that melatonin facilitates ETS1 deacetylation (Figure 4A). To identify the deacetylase involved, we employed pharmacological inhibitors. Pretreatment with the sirtuin inhibitor nicotinamide (NAM), but not the class I/II HDAC inhibitor trichostatin A (TSA), elevated ETS1 acetylation in melatonin-treated cells, suggesting the involvement of sirtuin family deacetylases (Figure 4B). Among the nuclear sirtuins tested (SIRT1, SIRT6, SIRT7), siRNA-mediated knockdown of SIRT1, but not SIRT6 or SIRT7, significantly increased ETS1 acetylation in melatonin-treated HPAEpiC cells (Figure 4C). Furthermore, endogenous co-immunoprecipitation assays revealed that melatonin enhanced the physical interaction between ETS1 and SIRT1 (Figure 4D), supporting a melatonin-regulated association under physiological conditions. Collectively, these results demonstrate that melatonin specifically promotes ETS1 deacetylation through SIRT1.

SIRT1-Mediated Deacetylation of ETS1 Is Essential for the Anti-Pyroptotic Effect of Melatonin

To determine whether SIRT1-dependent deacetylation of ETS1 regulates NLRP3 transcription, we performed knockdown of SIRT1. In melatonin-treated HPAEpiC cells, SIRT1 silencing resulted in a significant accumulation of nuclear ETS1 protein (Figure 5A) and a concomitant increase in NLRP3 mRNA levels (Figure 5B). Furthermore, ChIP analysis revealed enhanced binding of ETS1 to the NLRP3 promoter upon SIRT1 knockdown (Figure 5C). Compared to SIRT1 knockdown alone, the additional depletion of ETS1 in SIRT1-deficient cells markedly attenuated the increases in pyroptosis-related proteins (NLRP3, cleaved caspase-1, and GSDMD-N; Figure 5D), the percentage of PI-positive cells (Figure 5E), and the release of IL-1 β and IL-18 (Figure 5F). Collectively, these findings demonstrate that SIRT1-mediated deacetylation of ETS1 is a critical mechanism through which melatonin suppresses pyroptosis.

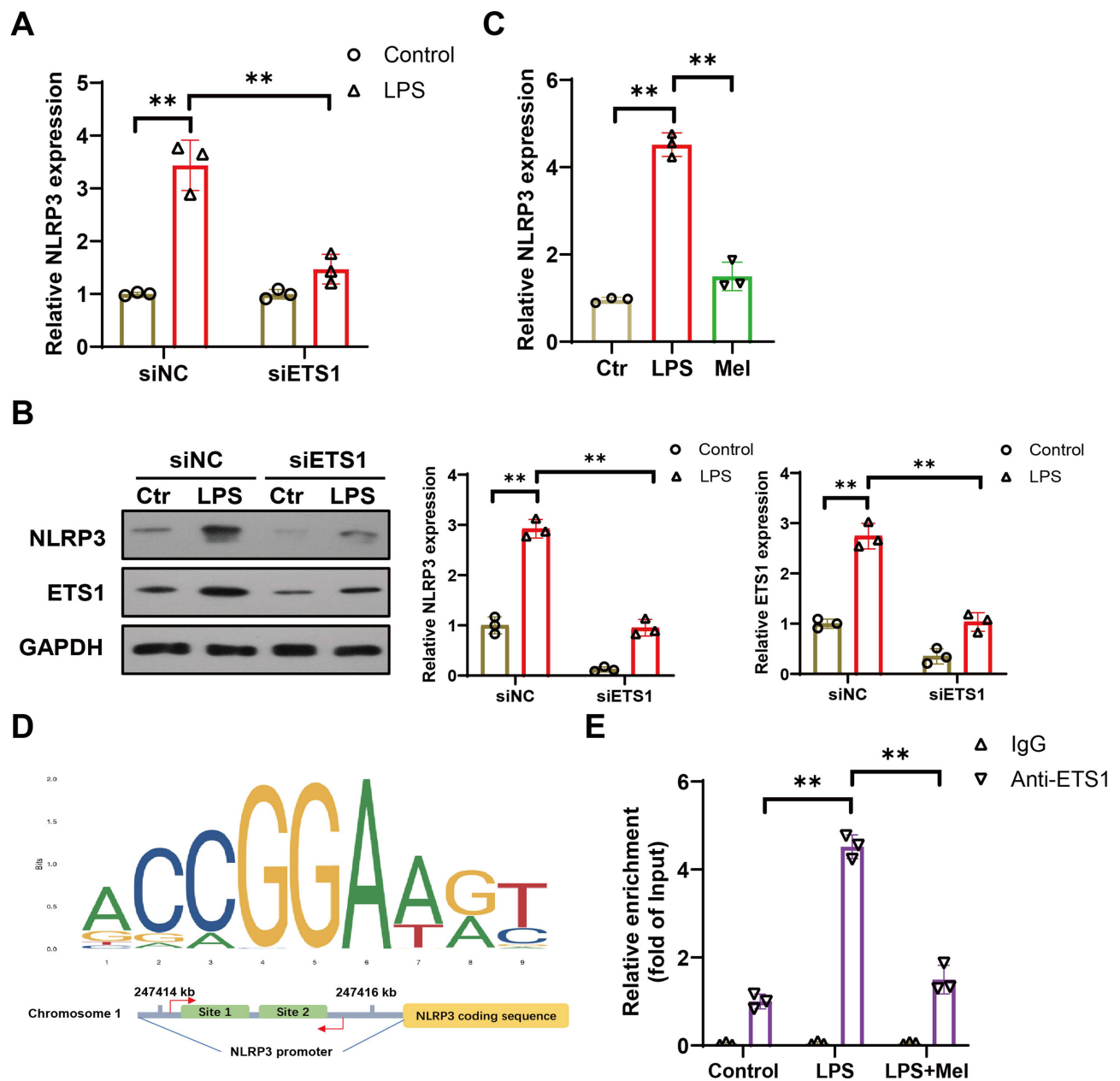


Figure 3 ETS1 directly regulates NLRP3 expression in melatonin-treated HPAEpiC cells. **(A and B)** RT-qPCR and Western blot analysis of NLRP3 mRNA and protein levels, respectively, in cells transfected with control siRNA (siNC) and ETS1 siRNA (siETS1). Data are shown as mean \pm SD. $n=3$ $**P<0.01$. Two-way ANOVA and Tukey's test. **(C)** RT-qPCR analysis of NLRP3 mRNA in control (ctr), LPS- or LPS + melatonin (Mel)-treated HPAEpiC cells. Data are shown as mean \pm SD. $n=3$. $**P<0.01$. One-way ANOVA and Tukey's test. **(D)** The predicted binding sites of ETS1 in the promoter of NLRP3. The primer sets for ChIP-qPCR are indicated by the red arrows in the schematic diagram. **(E)** ChIP-qPCR assessing ETS1 binding to the NLRP3 promoter in control (ctr), LPS- or LPS + melatonin (Mel)-treated HPAEpiC cells. Data are shown as mean \pm SD. $n=3$. $**P<0.01$. One-way ANOVA and Tukey's test. The scatter points (circles, triangles) on each data group of the bar chart represent individual data points.

MT2 Mediates Melatonin-Induced Activation of the SIRT1/ETS1/NLRP3 Axis and Suppression of Pyroptosis in LPS-Exposed HPAEpiC Cells

To identify the specific melatonin receptor responsible for its protective effects, we first verified the expression of MT1 and MT2 in HPAEpiC cells, with L-02 liver cells serving as a positive control (Figure 6A). Knockdown of MT2 using siRNA significantly attenuated the melatonin-induced upregulation of SIRT1 (Figure 6B) and the downregulation and deacetylation of ETS1 (Figure 6C) in LPS-treated cells. Consequently, MT2 silencing reversed the inhibitory effects of melatonin on pyroptosis. This was demonstrated by a decrease in cell viability (Figure 6D), increased protein levels of NLRP3, cleaved caspase-1, and GSDMD-N (Figure 6B), elevated releases of IL-1 β and IL-18 (Figure 6E), and a higher percentage of PI-

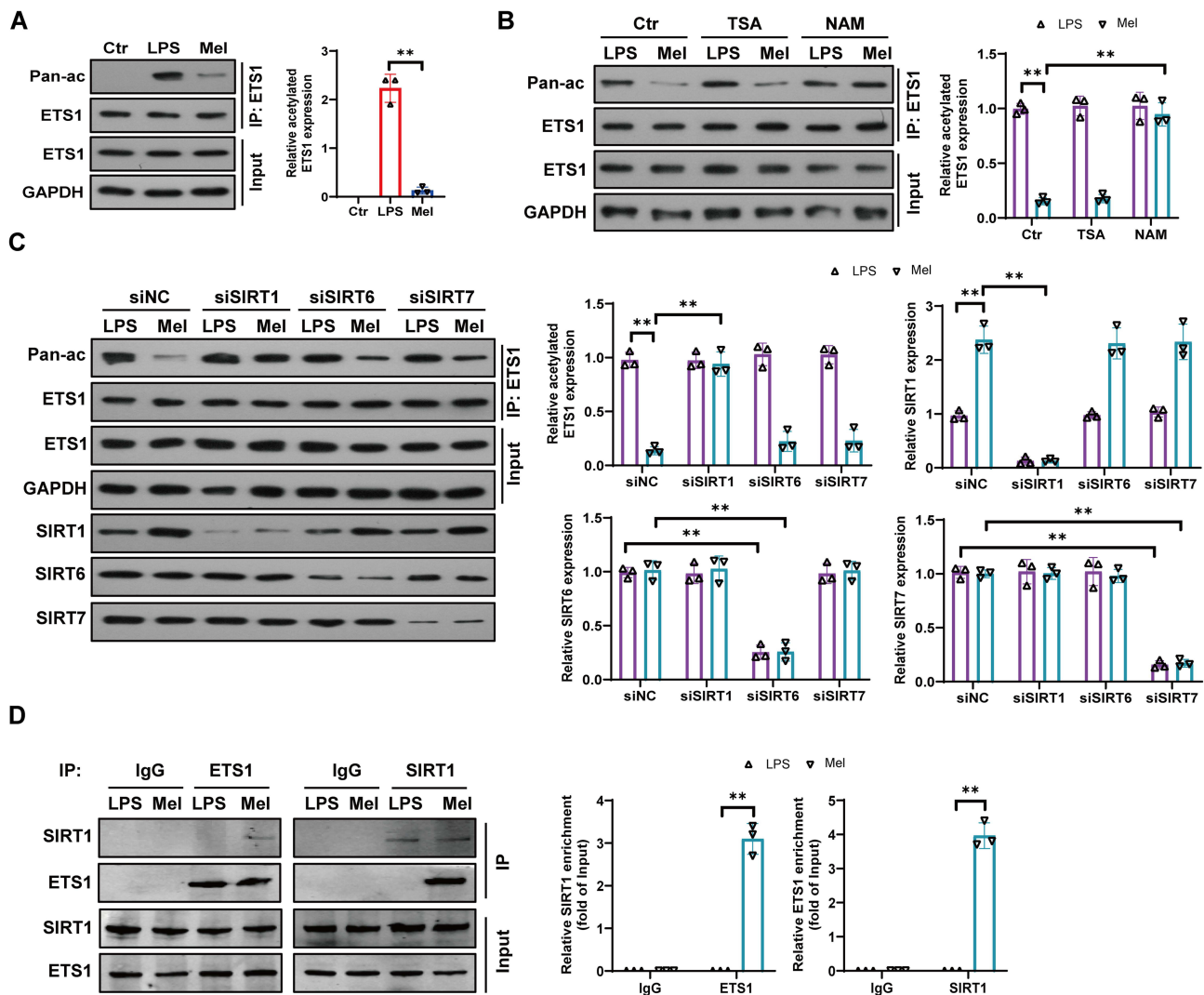


Figure 4 SIRT1 is required for melatonin-induced ETS1 deacetylation in the LPS-exposed HPAEpiC cells. **(A)** Immunoprecipitation (IP) analysis of acetylated levels of ETS1 in control (ctr), LPS- or LPS + melatonin (Mel)-treated HPAEpiC cells. Data are shown as mean \pm SD. $n=3$. $**P<0.01$. One-way ANOVA and Tukey's test. **(B)** IP analysis of acetylated levels of ETS1 in cells treated with LPS or LPS + melatonin (Mel), pretreated with NAM (10 mM) or TSA (1 μ M). Data are shown as mean \pm SD. $n=3$. $**P<0.01$. Two-way ANOVA and Tukey's test. **(C)** IP analysis of acetylated levels of ETS1 in cells treated with LPS or LPS + melatonin (Mel), transfected with control siRNA (siNC), SIRT1 siRNA (siSIRT1), SIRT6 siRNA (siSIRT6), and SIRT7 siRNA (siSIRT7). Data are shown as mean \pm SD. $n=3$. $**P<0.01$. Two-way ANOVA and Tukey's test. **(D)** Co-IP analysis of the interaction between SIRT1 and ETS1 in cells treated with LPS or LPS + melatonin (Mel). Data are shown as mean \pm SD. $n=3$. $**P<0.01$. Two-way ANOVA and Tukey's test. The scatter points (triangles) on each data group of the bar chart represent individual data points.

positive cells (Figure 6F). In contrast, MT1 knockdown did not significantly affect melatonin-induced SIRT1 upregulation (Figure 7A), ETS1 deacetylation (Figure 7B), or the suppression of pyroptosis markers (Figure 7C–E). Taken together, these results indicate that MT2, but not MT1, is essential for melatonin-mediated activation of the SIRT1/ETS1/NLRP3 pathway and the subsequent inhibition of pyroptosis in LPS-exposed HPAEpiC cells.

Discussion

This study reveals the molecular mechanisms underlying melatonin's mitigation of pyroptosis. We identified a specific signaling pathway mediating this anti-pyroptotic effect, as summarized in Figure 8. Specifically, we demonstrated that MT2, not MT1, is the primary melatonin receptor subtype activated in HPAEpiC cells. Upon MT2 activation, SIRT1 deacetylates ETS1, leading to suppression of NLRP3 inflammasome activation. Together, these findings demonstrate that melatonin inhibits LPS-induced pyroptosis in HPAEpiC cells via the MT2/SIRT1/ETS1/NLRP3 axis.

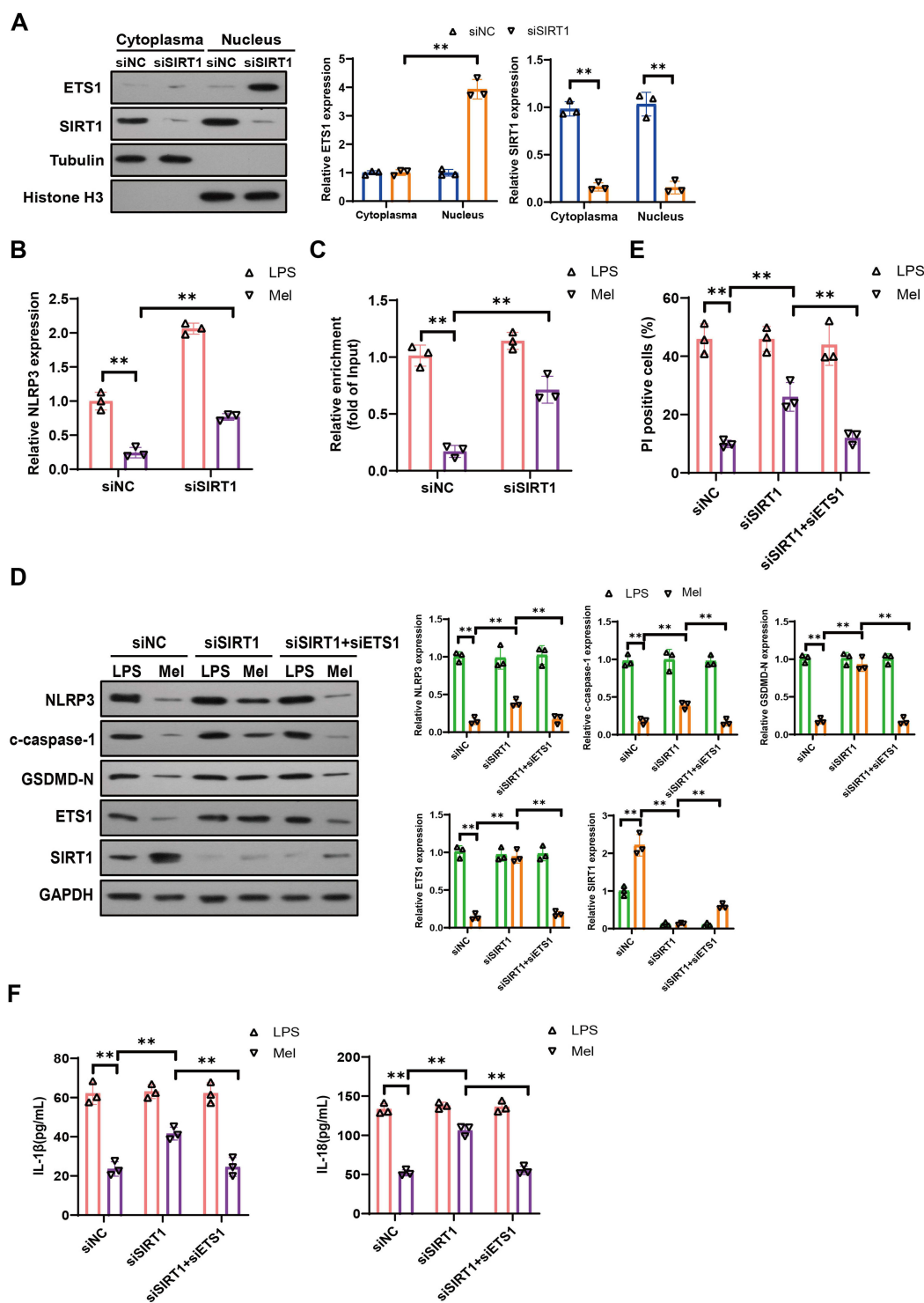


Figure 5 SIRT1-mediated ETS1 deacetylation is required for the anti-pyrototic effect of melatonin. **(A)** Western blot analysis of the location and expression of ETS1 in cells transfected with control siRNA (siNC) or SIRT1 siRNA (siSIRT1). Data are shown as mean \pm SD. $n=3$ $^{***}P<0.01$. Two-way ANOVA and Tukey's test. **(B)** RT-qPCR analysis of NLRP3 mRNA levels in cells treated with LPS or LPS + melatonin (Mel), transfected with control siRNA (siNC) and SIRT1 siRNA (siSIRT1). Data are shown as mean \pm SD. $n=3$ $^{***}P<0.01$. Two-way ANOVA and Tukey's test. **(C)** ChIP-qPCR assessing ETS1 binding to the NLRP3 promoter under the same conditions. Data are shown as mean \pm SD. $n=3$ $^{***}P<0.01$. Two-way ANOVA and Tukey's test. **(D)** Western blot analysis of NLRP3, c-caspase-1, and GSDMD-N in cells treated with LPS or LPS + melatonin (Mel), transfected with control siRNA (siNC), SIRT1 siRNA (siSIRT1), SIRT1 siRNA + ETS1 siRNA (siSIRT1 + siETS1). Data are shown as mean \pm SD. $n=3$ $^{***}P<0.01$. Two-way ANOVA and Tukey's test. **(E)** Hoechst33342/PI staining analysis of apoptosis under the same conditions. Data are shown as mean \pm SD. $n=3$ $^{***}P<0.01$. Two-way ANOVA and Tukey's test. **(F)** ELISA analysis of supernatant levels of IL-1 β and IL-18 in culture supernatants from the same experimental groups. Data are shown as mean \pm SD. $n=3$ $^{***}P<0.01$. Two-way ANOVA and Tukey's test. The scatter points (triangles) on each data group of the bar chart represent individual data points.

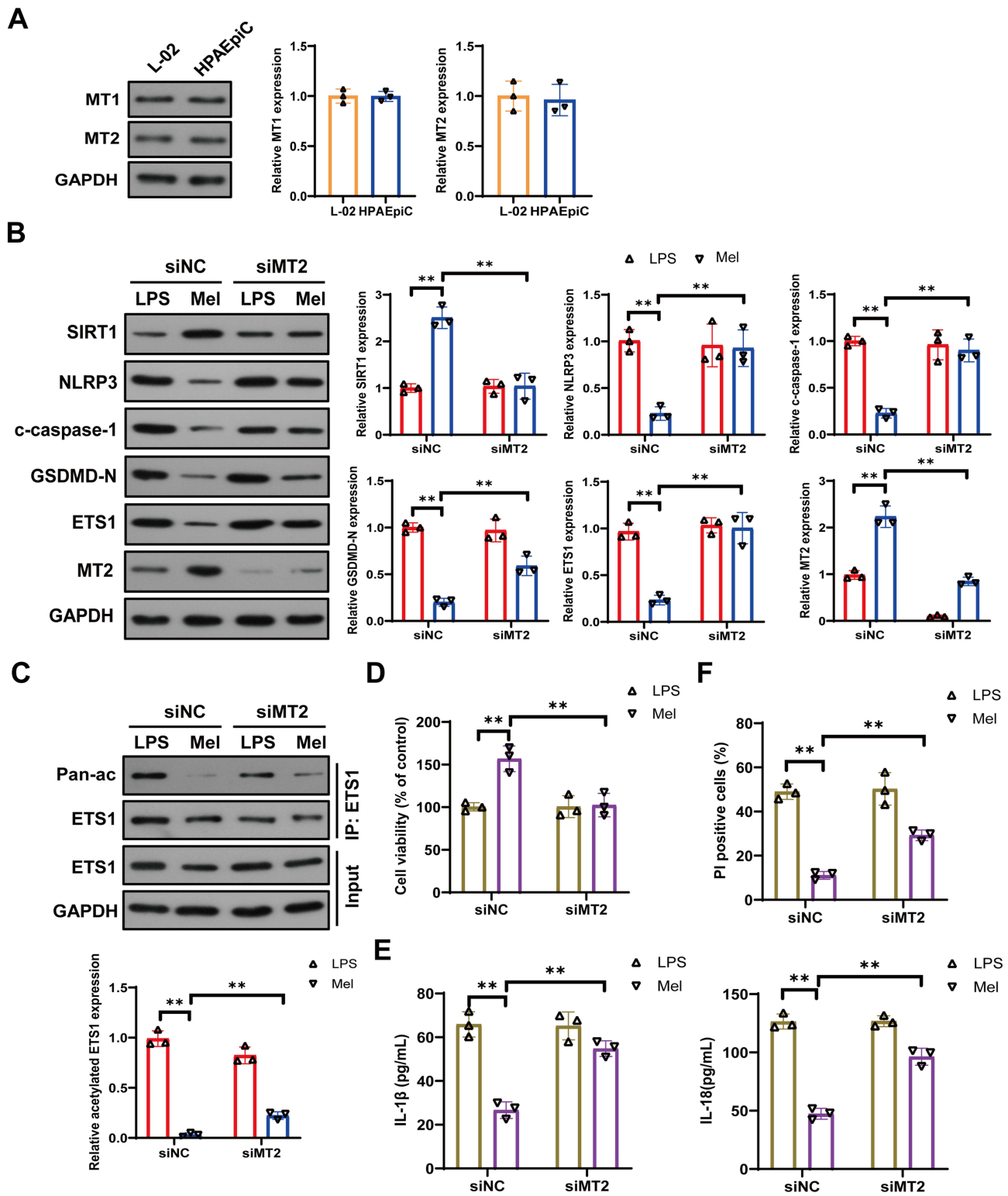


Figure 6 MT2 mediates the anti-pyroptotic effect of melatonin in the LPS-exposed HPAEpiC cells. **(A)** Western blot analysis of protein levels of MT1 and MT2 in L-02 cells and HPAEpiC cells. Data are shown as mean \pm SD. n=3. unpaired Student's two-tailed t-test. **(B)** Western blot analysis of MT2, ETS1, NLRP3, c-caspase-1, and GSDMD-N in cells treated with LPS or LPS + melatonin (Mel), transfected with control siRNA (siNC), or MT2 siRNA (siMT2). Data are shown as mean \pm SD. n=3 $**P<0.01$. Two-way ANOVA and Tukey's test. **(C)** IP analysis of acetylated levels of ETS1 under the same conditions. Data are shown as mean \pm SD. n=3 $**P<0.01$. Two-way ANOVA and Tukey's test. **(D)** CCK-8 analysis of cell viability under the same conditions. Data are shown as mean \pm SD. n=3 $**P<0.01$. Two-way ANOVA and Tukey's test. **(E)** ELISA analysis of supernatant levels of IL-1 β and IL-18 in culture supernatants from the same experimental groups. Data are shown as mean \pm SD. n=3 $**P<0.01$. Two-way ANOVA and Tukey's test. **(F)** Hoechst33342/PI staining analysis of apoptosis under the same conditions. Data are shown as mean \pm SD. n=3 $**P<0.01$. Two-way ANOVA and Tukey's test. Pan-ac, Pan-acetyl-lysine antibody. The scatter points (triangles) on each data group of the bar chart represent individual data points.

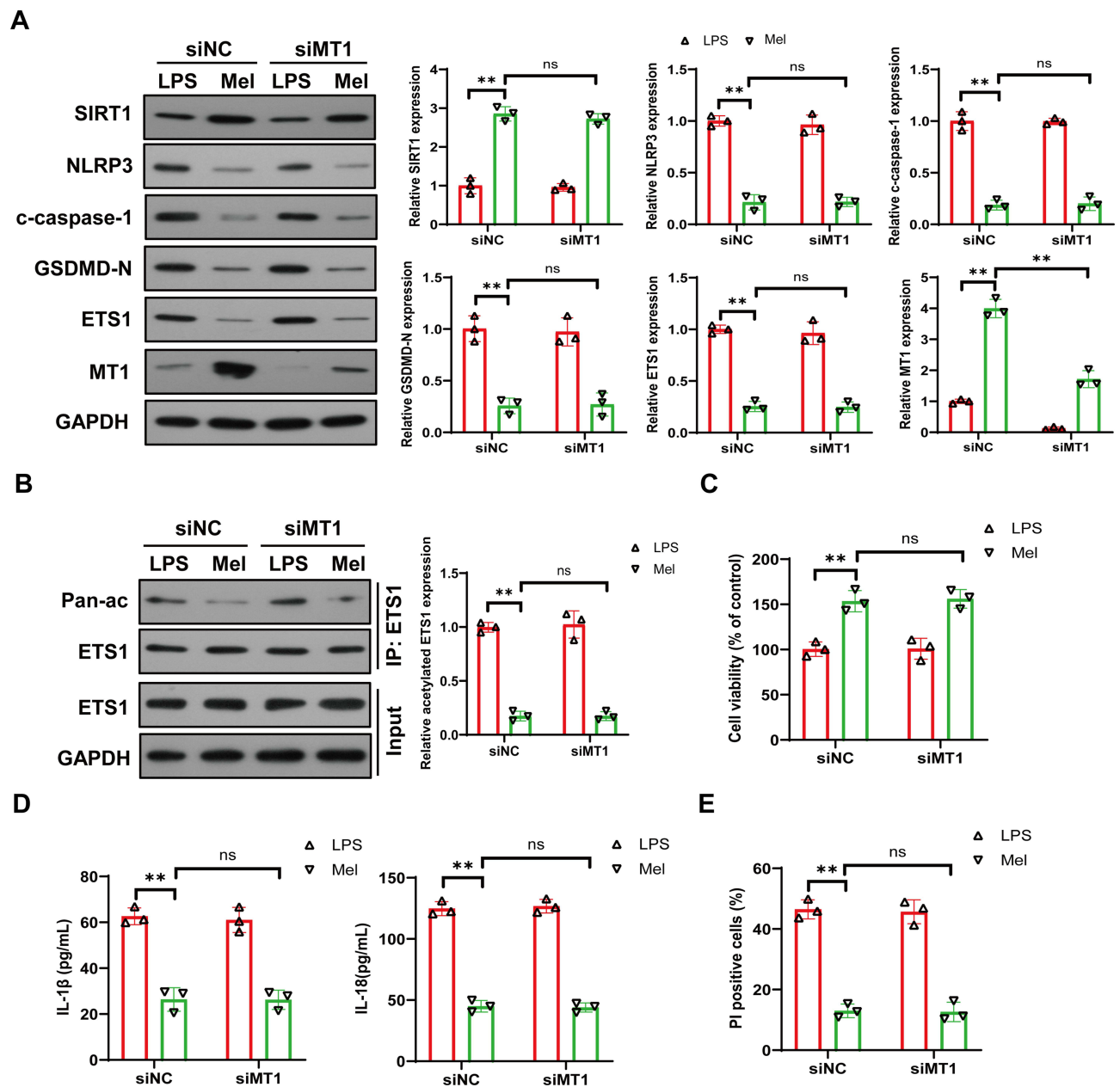


Figure 7 Effect of MT1 siRNA on the anti-pyroptotic effect of melatonin in the LPS-exposed HPAEpic cells. **(A)** Western blot analysis of MT1, ETS1, NLRP3, c-caspase-1, and GSDMD-N in cells treated with LPS or LPS + melatonin (Mel), transfected with control siRNA (siNC), or MT1 siRNA (siMT1). Data are shown as mean \pm SD. $n=3$ $^{**}P<0.01$. Two-way ANOVA and Tukey's test. **(B)** IP analysis of acetylated levels of ETS1 under the same conditions. Data are shown as mean \pm SD. $n=3$ $^{**}P<0.01$. Two-way ANOVA and Tukey's test. **(C)** CCK-8 analysis of cell viability under the same conditions. Data are shown as mean \pm SD. $n=3$ $^{**}P<0.01$. Two-way ANOVA and Tukey's test. **(D)** ELISA analysis of supernatant levels of IL-1 β and IL-18 in culture supernatants from the same experimental groups. Data are shown as mean \pm SD. $n=3$ $^{**}P<0.01$. Two-way ANOVA and Tukey's test. **(E)** Hoechst33342/PI staining analysis of apoptosis under the same conditions. Data are shown as mean \pm SD. $n=3$ $^{**}P<0.01$. Two-way ANOVA and Tukey's test. Pan-ac, Pan-acetyl-lysine antibody. The scatter points (triangles) on each data group of the bar chart represent individual data points.

Both in vitro and in vivo studies have established that melatonin mitigates NLRP3 inflammasome activity through multiple intracellular signaling pathways.^{25,26} For instance, Arioz et al showed that melatonin suppresses NLRP3 inflammasome activation and pyroptosis in murine microglia via the SIRT1/Nrf2 pathway.¹⁵ Similarly, Li et al recently reported that melatonin counteracts microglial pyroptosis and neuroinflammation by modulating the cGAS/STING/NF- κ B axis, thereby reshaping the immune microenvironment.²⁷ Additionally, Gao et al identified Cathepsin B as a target through which melatonin inhibits NLRP3-mediated pyroptosis in chronic stress-induced hippocampal microglia.²⁸ In contrast to these prior works, which largely focus on post-translational or signaling modulation of NLRP3 activation, our study reveals a previously

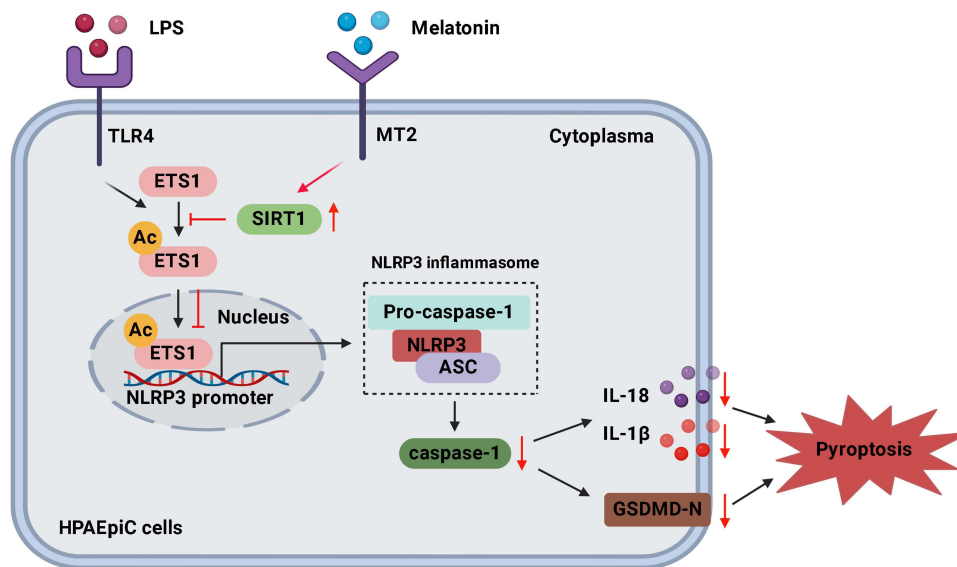


Figure 8 Schematic illustration of the proposed mechanism through which melatonin suppresses LPS-induced pyroptosis in HPAEpiC cells. Melatonin activates MT2 in HPAEpiC cells. Subsequent MT2 activation leads to SIRT1-mediated deacetylation of ETS1, thereby inhibiting NLRP3 inflammasome activation.

unexplored mechanism operating at the transcriptional level. We demonstrate that melatonin downregulates NLRP3 expression transcriptionally via the MT2/SIRT1/ETS1 axis, thereby fundamentally limiting the availability of core components necessary for inflammasome assembly and activation. This transcriptional regulation presents a novel and preventive dimension to melatonin's anti-pyroptotic actions, extending the current understanding of its therapeutic potential in inflammasome-driven pathologies.

A pivotal finding of this study is the identification of ETS1 as a key downstream effector through which melatonin inhibits pyroptosis in LPS-stimulated human pulmonary alveolar epithelial cells (HPAEpiCs). Our data demonstrate that melatonin attenuates the LPS-induced upregulation of ETS1. Crucially, the protective effect of melatonin against pyroptosis was significantly counteracted upon ETS1 overexpression, providing direct evidence for the necessity of ETS1 downregulation in melatonin's mechanism of action. This not only reinforces the established role of ETS1 in regulating pyroptosis and lung injury but also delineates a novel pathway by which melatonin confers protection.

Beyond transcriptional regulation, ETS1 function is extensively modulated by post-translational modifications (PTMs), which confer context-specific functional diversity. We further discovered that melatonin specifically reduces the acetylation level of ETS1, thereby diminishing its binding affinity to the NLRP3 promoter and ultimately attenuating pyroptosis. This finding aligns with the recognized role of acetylation in modulating ETS1 activity, as illustrated by its involvement in VEGF signaling through BRD4/P-TEFb interaction.²⁴ However, the functional outcome of ETS1 acetylation appears highly context-dependent. For instance, in contrast to our observation, p300-mediated acetylation promotes ETS1 dissociation from a promoter in glomerular mesangial cells.²⁹ In clear cell renal cell carcinoma (ccRCC) cells, HDAC8-induced deacetylation of ETS1 at K245 enhances the interaction between HIF-2 α and ETS1.³⁰ This disparity underscores the cell type- and stimulus-specific nature of PTM-mediated ETS1 regulation. Given that ETS1 activity is also governed by other PTMs such as phosphorylation (which enhances its stability and transcriptional activity³¹) and sumoylation (which represses activity without affecting degradation³²), an important future direction would be to investigate whether melatonin's regulation of ETS1 extends to these modifications, potentially revealing a broader, multi-faceted regulatory mechanism underlying its anti-pyroptotic effects.

Having established that melatonin reduces ETS1 acetylation to inhibit pyroptosis, we further identified SIRT1 as the pivotal deacetylase responsible for this effect. SIRT1, a class III histone deacetylase, is a well-recognized regulator of pyroptosis through the deacetylation of diverse substrates^{33,34} and a crucial downstream effector of melatonin in various contexts.^{14,15} Our data confirm that SIRT1-mediated deacetylation of ETS1 is indispensable for melatonin's anti-pyroptotic action in LPS-stimulated HPAEpiC cells. This extends the known repertoire of SIRT1 targets and delineates

a specific melatonin /SIRT1/ETS1(deacetylation)/pyroptosis axis in alveolar epithelium. Interestingly, melatonin has been reported to exert anti-pyroptotic effects in other cell types, such as cardiomyocytes and microglia, primarily through activating the SIRT1/Nrf2 signaling pathway.^{14,15} While our study highlights a direct SIRT1/ETS1 link, it remains to be investigated whether the SIRT1/Nrf2 axis operates concurrently or synergistically in our model. Future research should explore potential crosstalk between these pathways to determine if melatonin orchestrates a coordinated anti-pyroptotic program involving both transcription factor deacetylation (ETS1) and antioxidant signaling (Nrf2) in lung injury.

A particularly intriguing aspect of melatonin signaling is its receptor specificity across different biological contexts. Melatonin exerts many of its physiological effects by binding to its high-affinity G protein-coupled receptors, MT1 and MT2.^{35,36} However, the relative contribution of these receptors appears to be highly cell type- and injury-specific. While some studies report that both MT1 and MT2 mediate melatonin's anti-pyroptotic effects in auditory cells,¹⁶ others identify MT2 as the sole mediator in cardiomyocytes via a distinct miR-155/FOXO3a/ARC axis.¹⁷ In line with this notion of context dependency, our previous work in hyperoxia-exposed alveolar epithelial type II cells identified MT2, but not MT1, as the critical mediator of melatonin's anti-apoptotic effect via the PI3K/AKT/ETS1 pathway.²³ Extending this observation to pyroptosis, the present study demonstrates a similar receptor specificity. We found that knockdown of MT2, but not MT1, completely abolished melatonin's ability to inhibit LPS-induced pyroptosis and to promote SIRT1-mediated ETS1 deacetylation in HPAEpiC cells. These results establish a coherent signaling cascade from melatonin through MT2, leading to SIRT1 upregulation, ETS1 deacetylation, suppression of NLRP3 transcription, and ultimately inhibition of pyroptosis. This pathway not only consolidates the central role of MT2 in melatonin's pulmonary protective effects but also integrates the upstream receptor event with the downstream enzymatic (SIRT1) and transcriptional (ETS1) mechanisms we have elucidated. To further solidify the central role of MT2, future experiments will employ the MT2-selective antagonist 4P-PDOT to pharmacologically block the receptor, and will utilize CRISPR-Cas9-generated MT2 knockout cell lines to confirm the genetic necessity of MT2 in this signaling axis. A key question arising from our findings is what governs this receptor specificity. Whether it stems from differential receptor expression, unique coupling to downstream effectors, or crosstalk with other injury-specific signals in alveolar epithelium warrants further investigation.

While this study provides valuable mechanistic insights into the inhibitory effects of melatonin on pyroptosis, several limitations should be acknowledged. First, our conclusions are primarily based on *in vitro* cell models, and further *in vivo* validation is needed to substantiate the anti-pyroptotic efficacy of melatonin. To directly evaluate the clinical relevance of the proposed pathway, future studies could analyze publicly available transcriptomic datasets (eg, from GEO) of relevant human lung diseases, examining whether expression levels of MT2, SIRT1, ETS1, and NLRP3 correlate with disease severity or clinical outcomes. Additionally, collaborative clinical investigations could assess whether protein levels or activity states (eg, ETS1 acetylation) of these pathway components in patient-derived bronchoalveolar lavage fluid or lung biopsies are associated with inflammatory status or therapeutic response. Second, the research focused exclusively on HPAEpiC cells; thus, the influence of melatonin on other relevant lung cell types during injury remains unexplored. Future work should therefore examine its effects in additional cellular and preclinical models to better delineate its cell-type-specific actions and therapeutic potential. Third, although our findings highlight the importance of the MT2/SIRT1/ETS1/NLRP3 axis, other molecular mechanisms likely contribute to melatonin-mediated regulation of LPS-induced pyroptosis. Investigating these unexplored pathways will be an important direction for subsequent research.

Conclusion

In conclusion, this study identifies the MT2/SIRT1/ETS1/NLRP3 axis as a crucial pathway mediating the anti-pyroptotic effects of melatonin in LPS-stimulated HPAEpiC cells. These findings not only elucidate a novel mechanism underlying melatonin's anti-inflammatory action but also highlight its therapeutic potential for inflammation-associated lung diseases. Future translational research should focus on validating this axis in relevant preclinical models and evaluating its potential as a druggable target. Investigating possible synergies between targeting this pathway and existing anti-inflammatory or anti-pyroptosis therapies could inform novel combination strategies. Further exploration of additional mechanisms contributing to melatonin's protection against LPS-induced pyroptosis remains warranted.

Abbreviations

HPAEpiC, Human pulmonary alveolar epithelial cells; LPS, Lipopolysaccharide; ETS1, E26 oncogene homolog 1; ChIP, Chromatin immunoprecipitation; NLRP3, NLR family of pyrin domains containing 3; SIRT1, sirtuin 1; MT2, Melatonin receptor 2; GSDMD, gasdermin D; IL-18, Interleukin-18; IL-1 β , Interleukin-1 β ; AD, Alzheimer's disease; PTMs, Post-translational modifications; P-TEFb, Positive Transcription Elongation Factor-b; BRD4, Bromodomain-containing protein 4; Nrf2, E2-associated factor 2; OGD/R, Oxygen-glucose deprivation/reperfusion; HEI-OC1, House Ear Institute-Organ of Corti 1; FOXO3a, Forkhead box O3a; ARC, Caspase recruitment domain; AECIIs, Alveolar epithelial type II cells.

Data Sharing Statement

The datasets used and/or analyzed during the study are available from the corresponding author upon reasonable request.

Author Contributions

Fan He: Writing-review & editing, Writing- original draft, Methodology, Investigation, Conceptualization. Chunzi Liu: Writing-review & editing, Investigation, Conceptualization. Yun Yu: Writing-review & editing, Investigation, Conceptualization. Qiaofang Wang: Writing-review & editing, Resources, Investigation, Data Curation. Lin Li: Writing-review & editing, Resources, Methodology, Validation. Xaioyun Chao: Writing-review & editing, Resources, Formal analysis, Project administration. Liping Chen: Conceptualization, Supervision, Writing-review & editing. Cong Yu: Writing-original draft, Supervision, Project administration, Funding acquisition, Conceptualization. All authors read and approved the final manuscript. All authors have agreed on the journal to which the article has been submitted; and agree to be accountable for all aspects of the work.

Funding

This work was supported by the Jiangxi Provincial Children's Hospital Qingmiao Research Fund (2024JXEYQM10), Jiangxi Provincial Health Technology Project (202610767, 202610774).

Disclosure

The authors declare that there are no competing interests.

References

- Shen X, He L, Cai W. Role of lipopolysaccharides in the inflammation and pyroptosis of alveolar epithelial cells in acute lung injury and acute respiratory distress syndrome. *J Inflamm Res.* 2024;17:5855–5869. doi:10.2147/JIR.S479051
- Jia G, Song E, Zheng Z, Qian M, Liu G. Alveolar epithelial cells in bacterial sepsis-associated acute lung injury: mechanisms and therapeutic strategies. *Front Immunol.* 2025;16:1605797. doi:10.3389/fimmu.2025.1605797
- Wan H, Zhang Y, Gao Z, Shan G, Yin J, Li H. Procyanidin B2 alleviates LPS-induced acute lung injury by regulating M1 macrophage polarization and inhibiting pyroptosis via the NF-kappaB/JAK2/STAT1 signaling pathway. *Eur J Pharmacol.* 2025;1006:178149. doi:10.1016/j.ejphar.2025.178149
- Liu Y, Shang L, Zhou J, Pan G, Zhou F, Yang S. Emodin attenuates LPS-induced acute lung injury by inhibiting NLRP3 inflammasome-dependent pyroptosis signaling pathway in vitro and in vivo. *Inflammation.* 2022;45(2):753–767. doi:10.1007/s10753-021-01581-1
- Shan M, Wan H, Ran L, et al. Dynasore alleviates LPS-induced acute lung injury by inhibiting NLRP3 inflammasome-mediated pyroptosis. *Drug Des Devel Ther.* 2024;18:1369–1384. doi:10.2147/DDDT.S444408
- Wang J, Li LL, Zhao ZA, Niu CY, Zhao ZG. NLRP3 inflammasome-mediated pyroptosis in acute lung injury: roles of main lung cell types and therapeutic perspectives. *Int Immunopharmacol.* 2025;154:114560. doi:10.1016/j.intimp.2025.114560
- Zhang C, Chen X, Wei T, et al. Xuebijing alleviates LPS-induced acute lung injury by downregulating pro-inflammatory cytokine production and inhibiting gasdermin-E-mediated pyroptosis of alveolar epithelial cells. *Chin J Nat Med.* 2023;21(8):576–588. doi:10.1016/S1875-5364(23)60463-7
- Xie WM, Su W, Liu XY, et al. FTO deficiency alleviates LPS-induced acute lung injury by TXNIP/NLRP3-mediated alveolar epithelial cell pyroptosis. *Am J Respir Cell Mol Biol.* 2024;70(5):351–363. doi:10.1165/rcmb.2023-02510C
- Chitimus DM, Popescu MR, Voiculescu SE, et al. Melatonin's impact on antioxidative and anti-inflammatory reprogramming in homeostasis and disease. *Biomolecules.* 2020;10(9):1211. doi:10.3390/biom10091211
- Yousefi B, Reiter RJ. Melatonin in health and diseases. *Biochimie.* 2022;202:1. doi:10.1016/j.biochi.2022.10.003
- de Matos Cavalcante AG, de Bruin PF, de Bruin VM, et al. Melatonin reduces lung oxidative stress in patients with chronic obstructive pulmonary disease: a randomized, double-blind, placebo-controlled study. *J Pineal Res.* 2012;53(3):238–244. doi:10.1111/j.1600-079X.2012.00992.x
- Chen YT, Chiang HJ, Chen CH, et al. Melatonin treatment further improves adipose-derived mesenchymal stem cell therapy for acute interstitial cystitis in rat. *J Pineal Res.* 2014;57(3):248–261. doi:10.1111/jpi.12164
- Kang JY, Xu MM, Sun Y, et al. Melatonin attenuates LPS-induced pyroptosis in acute lung injury by inhibiting NLRP3-GSDMD pathway via activating Nrf2/HO-1 signaling axis. *Int Immunopharmacol.* 2022;109:108782. doi:10.1016/j.intimp.2022.108782

14. Zhang W, Wang X, Tang Y, Huang C. Melatonin alleviates doxorubicin-induced cardiotoxicity via inhibiting oxidative stress, pyroptosis and apoptosis by activating Sirt1/Nrf2 pathway. *Biomed Pharmacother.* 2023;162:114591. doi:10.1016/j.biopha.2023.114591
15. Arioz BI, Tastan B, Tarakcioglu E, et al. Melatonin attenuates LPS-induced acute depressive-like behaviors and microglial NLRP3 inflammasome activation through the SIRT1/Nrf2 pathway. *Front Immunol.* 2019;10:1511. doi:10.3389/fimmu.2019.01511
16. Zheng Y, Gao N, Zhang W, et al. Melatonin alleviates the oxygen-glucose deprivation/reperfusion-induced pyroptosis of HEI-OC1 cells and cochlear hair cells via MT-1,2/Nrf2 (NFE2L2)/ROS/NLRP3 pathway. *Mol Neurobiol.* 2023;60(2):629–642. doi:10.1007/s12035-022-03077-x
17. Chen R, Yang M. Melatonin inhibits OGD/R-induced H9c2 cardiomyocyte pyroptosis via regulation of MT2/miR-155/FOXO3a/ARC axis. *Int Heart J.* 2022;63(2):327–337. doi:10.1536/ihj.21-571
18. Yang M, Gao XR, Meng YN, Shen F, Chen YP. ETS1 ameliorates hyperoxia-induced alveolar epithelial cell injury by regulating the TGM2-mediated Wnt/beta-catenin pathway. *Lung.* 2021;199(6):681–690. doi:10.1007/s00408-021-00489-9
19. Shaik S, Maegawa S, Haltom AR, et al. REST promotes ETS1-dependent vascular growth in medulloblastoma. *Mol Oncol.* 2021;15(5):1486–1506. doi:10.1002/1878-0261.12903
20. Yan M, Komatsu N, Muro R, et al. ETS1 governs pathological tissue-remodeling programs in disease-associated fibroblasts. *Nat Immunol.* 2022;23(9):1330–1341. doi:10.1038/s41590-022-01285-0
21. Tai TS, Tsao HW, Chuang WC, et al. Ets1 regulates the differentiation and function of iNKT cells through both Pointed domain-dependent and domain-independent mechanisms. *Cell Mol Immunol.* 2020;17(11):1198–1200. doi:10.1038/s41423-020-0382-2
22. Juan C, Zhu Y, Chen Y, et al. Knocking down ETS Proto-oncogene 1 (ETS1) alleviates the pyroptosis of renal tubular epithelial cells in patients with acute kidney injury by regulating the NLR family pyrin domain containing 3 (NLRP3) transcription. *Bioengineered.* 2022;13(5):12927–12940. doi:10.1080/21655979.2022.2079242
23. He F, Wang QF, Li L, et al. Melatonin protects against hyperoxia-induced apoptosis in alveolar epithelial type II cells by activating the MT2/PI3K/AKT/ETS1 signaling pathway. *Lung.* 2023;201(2):225–234. doi:10.1007/s00408-023-00610-0
24. Chen J, Fu Y, Day DS, et al. VEGF amplifies transcription through ETS1 acetylation to enable angiogenesis. *Nat Commun.* 2017;8(1):383. doi:10.1038/s41467-017-00405-x
25. Ashrafizadeh M, Najafi M, Kavyiani N, Mohammadinejad R, Farkhondeh T, Samarghandian S. Anti-inflammatory activity of melatonin: a focus on the role of NLRP3 inflammasome. *Inflammation.* 2021;44(4):1207–1222. doi:10.1007/s10753-021-01428-9
26. Arioz BI, Tarakcioglu E, Olcum M, Genc S. The role of melatonin on NLRP3 inflammasome activation in diseases. *Antioxidants.* 2021;10(7):1020. doi:10.3390/antiox10071020
27. Li Q, Feng L, Tian Y, et al. Melatonin alleviates neuroinflammation in ischemic stroke by regulating cGAS-mediated microglial pyroptosis signaling. *Neural Regen Res.* 2025. doi:10.4103/NRR.NRR-D-24-01070
28. Gao Z, Luo K, Hu Y, et al. Melatonin alleviates chronic stress-induced hippocampal microglia pyroptosis and subsequent depression-like behaviors by inhibiting Cathepsin B/NLRP3 signaling pathway in rats. *Transl Psychiatry.* 2024;14(1):166. doi:10.1038/s41398-024-02887-y
29. Kato M, Dang V, Wang M, et al. TGF-beta induces acetylation of chromatin and of Ets-1 to alleviate repression of miR-192 in diabetic nephropathy. *Sci Signal.* 2013;6(278):ra43. doi:10.1126/scisignal.2003389
30. Qian K, Li W, Ren S, et al. HDAC8 enhances the function of HIF-2alpha by deacetylating ETS1 to decrease the sensitivity of TKIs in ccRCC. *Adv Sci.* 2024;11(36):e2401142. doi:10.1002/advs.202401142
31. Dhara A, Aier I, Das S, et al. Enhanced ETS1 stability by DNAPKcs orchestrates transcriptional changes during chemoresistance in triple negative breast cancer. *NPJ Breast Cancer.* 2025;11(1):114. doi:10.1038/s41523-025-00782-3
32. Ji Z, Degerny C, Vintonenko N, et al. Regulation of the Ets-1 transcription factor by sumoylation and ubiquitylation. *Oncogene.* 2007;26(3):395–406. doi:10.1038/sj.onc.1209789
33. Kadono K, Kageyama S, Nakamura K, et al. Myeloid Ikaros-SIRT1 signaling axis regulates hepatic inflammation and pyroptosis in ischemia-stressed mouse and human liver. *J Hepatol.* 2022;76(4):896–909. doi:10.1016/j.jhep.2021.11.026
34. Ma Z, Tang P, Dong W, et al. SIRT1 alleviates IL-1beta induced nucleus pulposus cells pyroptosis via mitophagy in intervertebral disc degeneration. *Int Immunopharmacol.* 2022;107:108671. doi:10.1016/j.intimp.2022.108671
35. Stauch B, Johansson LC, Cherezov V. Structural insights into melatonin receptors. *FEBS J.* 2020;287(8):1496–1510. doi:10.1111/febs.15128
36. Cecon E, Liu L, Jockers R. Melatonin receptor structures shed new light on melatonin research. *J Pineal Res.* 2019;67(4):e12606. doi:10.1111/jpi.12606